Front. Chem. China 2009, 4(3): 278–291
DOI 10.1007/s11458-009-0088-6

RESEARCH ARTICLE

Address-crossing digital information processing on a self-aggregatable cyclodextrin derivative based nanosystem

Liangliang ZHU, Fengyuan JI, Qiaochun WANG, Xiang MA, Zhaofei CHEN and He TIAN (✉)

A novel pH-responsive and photo-isomerizing *β*-cyclodextrin (*β*-CD) derivative DACD was synthesized and fully characterized by ^{1}H-NMR, ^{13}C-NMR, and HRMS. At room temperature, this compound would self-assemble to layer aggregations in an aqueous environment. The aggregated state can reversibly switch to a monomeric solution state attributed to the hydrophobic competition of an additional substance to the *β*-CD cavity. This self-aggregatable cyclodextrin derivative based nanosystem functioned by switching between the aggregated and monomeric state. An effective address-crossing digital information system, in response to pH and UV stimuli, was demonstrated based on such mechanism. This chemical system, capable of data memories and logic functions in nanoscale, can mimic the functions of pointer-based data processing.

Keywords supramolecular assembly, aggregation, memory address, logic gate

1 Introduction

The growing diversity of artificial supramolecular nanomaterials [1–4] provides choices and references for devising new-style digital information processing systems [5–8]. Cyclodextrins (CDs) and their derivatives [9–12] with multi-state switching and multi-responsive properties are ideal candidates for molecular logic storage. Hitherto, a large number of chemical or biological systems performing versatile functions of digital electronic components [13–22] have been demonstrated in nanoscale spaces or *in vivo*. However, the utilization of either the stable aggregated or the monomeric conformational species, which are generated by reversible supramolecular assembly and disassembly behavior as addressed media of data storage and logic calculations, is rarely reported. Moreover, the switching between the aggregated and monomeric state is a new information technique for the whole continuum of digital systems at the molecular level because it takes advantage of simple chemical operations for separated information writing and reading. Here we presented a memory address-crossing digital information switching system in nanoscale. The recorded pH and UV data can be read out as optical signatures with different logic performances, which can mimic the functions of pointer-based data processing and management in computer science.

Received March 18, 2009; accepted April 17, 2009
Key Laboratory for Advanced Materials and Institute of Fine Chemicals, East China University of Science & Technology, Shanghai 200237, China
E-mail: tianhe@ecust.edu.cn

2 Experimental section

2.1 Instruments

^{1}H-NMR, ^{13}C-NMR, and 2D-ROESY NMR spectra were measured on a Brüker AV-400 and an AV-500 spectrometer with tetramethylsilane (TMS) as internal standard. The high-resolution electrospray ionization mass spectrum (ESI) was recorded on a HP5989 mass spectrometer. Absorption spectra were performed on a Varian Cary 500 UV/Vis spectrophotometer (1 cm quartz cell was used). The transmission electric microscopy was carried out on a JEOL-JEM2100F electron microscope. The particle-size analysis was performed on a LS230 laser diffraction particle size analyzer. The X-ray diffraction was performed with a D/MAX 2550 VB/PC polycrystal X-ray diffractometer. The ICD spectra were recorded on a Jasco J-815 CD spectrophotometer in a 1 cm quartz cell. Fluorescent spectra were recorded on a Varian Cary Eclipse fluorescence spectrophotometer. The pH values were measured by using a PHS-3C pH meter. Photoirradiation was carried out on a CHF-XM 500-W high-pressure mercury lamp with a filter at 380 nm in a sealed Ar-saturated 1 cm quartz cell. The distance between the lamp and the sample cell was 20 cm. Melting points were determined by using an X-6 micro-melting point apparatus.

2.2 Materials

2-(4-hydroxyphenyl)acetonitrile, *β*-cyclodextrin (*β*-CD), 4-dimethylamino benzaldehyde, and p-toluenesulfonyl chloride were commercially available and used without further purification. 1,8-diazabicyclo[5.4.0]undec-7-ene (DBU) and 1-Adamantanol (1-Ada) were purchased from Alfa Aesar and used as received. Pyridine and dimethyl formamide (DMF) were dried over potassium hydroxide and calcium hydride,

© Higher Education Press and Springer-Verlag 2009

respectively, and then distilled under reduced pressure. Tetrahydrofuran (THF) was refluxed over sodium particles and distilled before used.

2.3 Preparation of DACD

To a solution of DMF (15 mL) containing compound B (see Scheme 1, 1.0 g, 0.776 mmol) and potassium carbonate (0.2 g, 1.45 mmol), compound A2 (0.274 g, 1.037 mmol) was added. The resultant mixture was stirred at 90°C for 4 days under argon. The solution was poured into 80 mL THF; the precipitate was then collected by filtration to yield a yellow powder. The crude product was washed with hot water (100 mL) and then applied to silica gel chromatography (n-butanol : ethanol : water = 5∶4∶3) to generate a pure sample (0.61 g, 57%). M.p. > 250°C. ^{1}H-NMR (400 MHz, DMSO-d6, 25°C, TMS): δ = 7.78 (d, J = 8.8 Hz, 2 H), 7.61 (s, 1 H), 7.54 (d, J = 8.8 Hz, 2 H), 7.01 (d, J = 8.8 Hz, 2 H), 6.76 (d, J = 8.6 Hz, 2 H), 5.71–5.84 (m, 14 H), 4.80–4.86 (m, 7 H), 4.54–4.64 (m, 5 H), 4.20 (m, 3 H), 3.15–3.72 (m), 2.97 (s, 6 H). HRMS (ESI) : m/z: 1403.4768 $[DACD + Na]^+$.

3 Results and discussion

3.1 Aggregation and disassembly of DACD in aqueous environment

DACD comprises a D-π-A fluorophore linked covalently to the 6 position of *β*-CD (Figure 1). Each moiety of this molecule has its unique function. Besides the fluorescence (FL) emission performance of DACD itself, the inclusion effect of the chiral cyclodextrin cavity, the protonation of the dimethylamino unit, and the photoisomerization of the cyanostilbene unit are attractive features for the construction of a novel digital switching system.

DACD has a good solubility and exists in a dissociated state in some organic solvents such as DMF or dimethyl sulphoxide (DMSO). In this case, the solvation brings the D-π-A fluorophore far out of the cyclodextrin host, so that the NOEs of the protons between the aromatic regions and *β*-CD are hardly observed in the NMR spectra. On the contrary, an opaque colloidal system forms when DACD is dispersed in an aqueous environment at room temperature. Such system is observed by light scattering phenomenon (a 532 nm laser beam) and strong induced circular dichroism (ICD) signals compared with the solution state in DMF or DMSO. Unfortunately, 2D ROESY NMR does not provide useful information because DACD is sparingly soluble in water. But the generation of sharp ICD signals [23] indicates that the fluorophore has entered the chiral host of *β*-CD due to the hydrophobic inclusion effect of the cyclodextrin cavity. The image of the transmission electric microscopy (TEM, Figure 1) and the particle-size distribution with an intensity-mean 387.2 nm (see Supporting Information, Figure A6) show that the aggregated state is generally formed in water. The shapes and angular positions of the main peaks, numeral marked in the X-ray powder diffraction (XRD) pattern (see

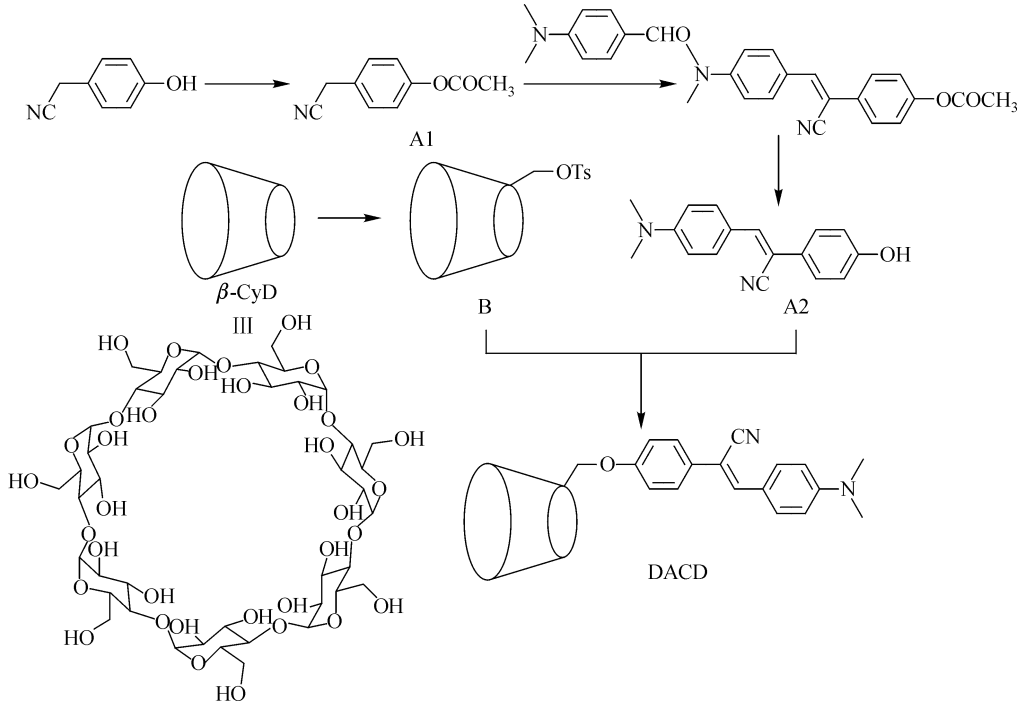

Scheme 1 Synthetic route to DACD.

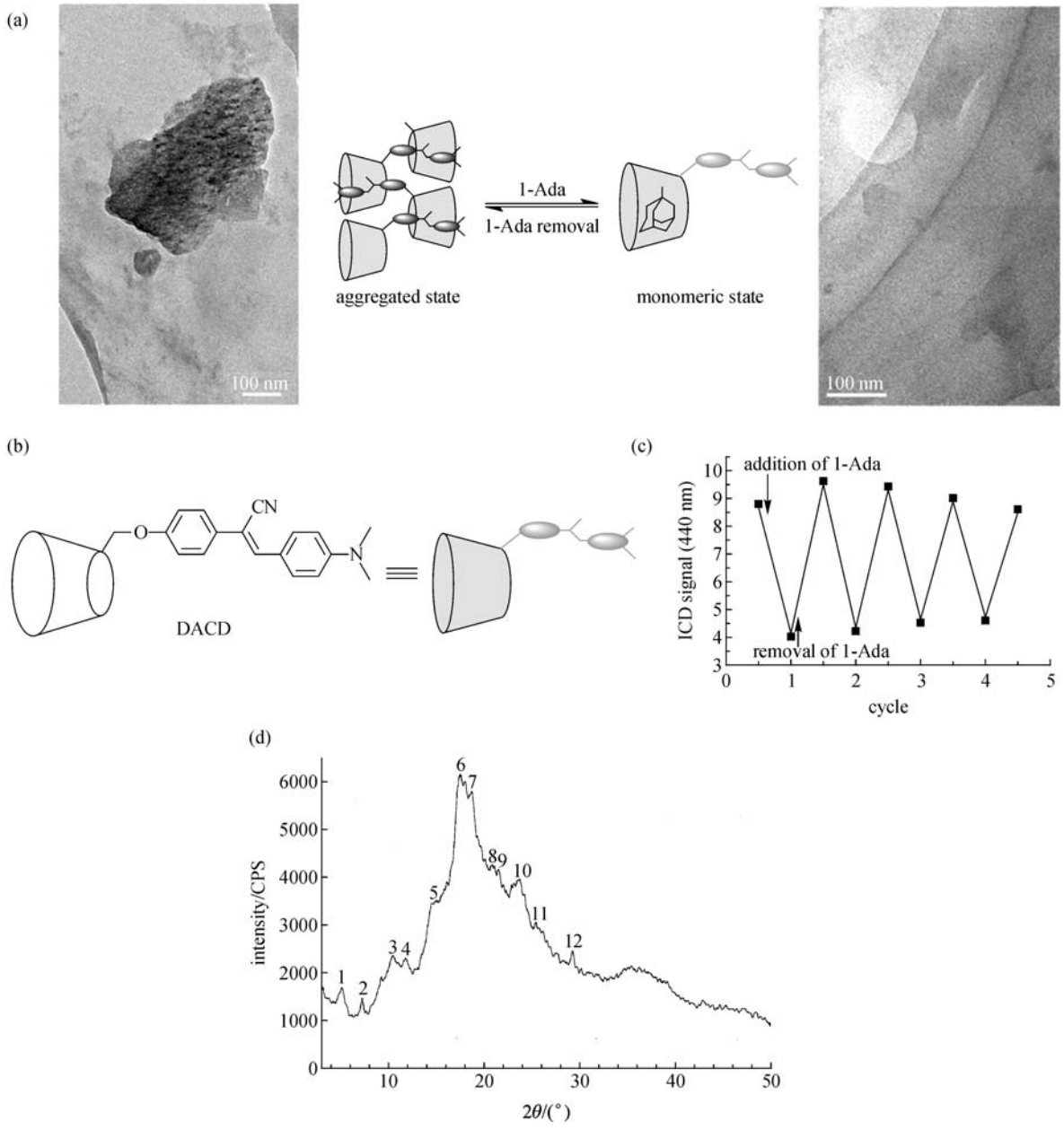

Figure 1 (a) TEM images describing the switching between the aggregated and monomeric state (b) the compound DACD (c) changes in ICD signals at 440 nm of DACD (3.0×10^{-5} mol/L) in water at 288 K along with the alternations induced by adding 1-Ada and removing it (d) the X-ray diffraction (XRD) spectrum of DACD. The solid sample was prepared from the aggregated state in water.

Figure 1) for DACD, indicate a layer structure in the aggregation. 1-Ada is a common competitive substance for replacing other guests in the β-CD cavity. The addition of 5 mol equivalents of 1-Ada to the initial system would extrude the fluorophore from the β-CD cavity to form a dissociate solution due to a higher association constant ($K = 1.09 \times 10^4$ (mol/L)$^{-1}$) between the host and the 1-Ada guest. The aggregation hence disassembled. This phase transition is reversible since 1-Ada can be removed by the extraction of organic solvents to recover the aggregated state [24].

3.2 Conformational-form transformations of DACD in aqueous environment

The addition of proton and light irradiation at 380 nm are two propulsions driving the compound to another two inter-convertible forms in the aggregated state. These two stimuli can also work for the 1-Ada triggered monomeric state, resulting in corresponding conformational stable forms. The conformational-form transformations of DACD in an aqueous environment are shown in Scheme 2, and the absorption

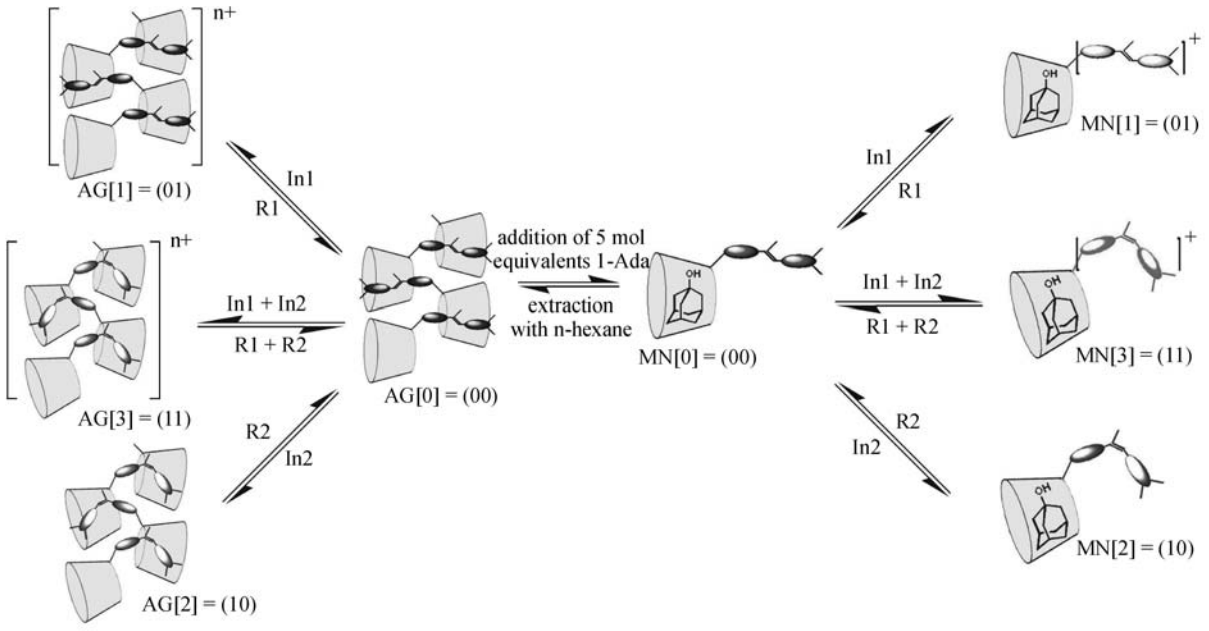

Scheme 2 Self-aggregate and disassembly as well as conformational-form transformations of DACD in water responding to multiple stimuli (Operations: In1: Adjustment of pH to below 0.7 with concentrated HCl; In2: Sufficient irradiation at 380 nm; R1: Neutralization with NaOH; R2: Heating).

spectra for each stable state are displayed in Figure 2. It is speculated that the protonation of the dimethylamino unit moved the chemical shifts of protons in the aromatic regions near the aminium to a lower field in the NMR spectra due to the deshielding effect of the aminium (see Supporting Information, Figure A7). In the initial state, the cyanostilbene unit exists almost in Z-form. Sufficient irradiation at 380 nm to the initial conformation can induce the photoisomerization of the cyanostilbene unit to E-form. With a photoisomerization efficiency of 70%, another cluster of peaks of the aromatic protons arises in the ^{1}H-NMR spectrum (see Supporting Information, Figure A7). The full loading of the above two stimuli onto the initial system in water lead to another two aggregated forms. The shrinkage of the primary D-π-A conjugated system [25, 26] in the AG[1] aggregated form causes the original maximum absorption to decrease, while a new absorption peak appears at 345 nm. On the other hand, a low molar absorption coefficient of E-form in the AG [2] aggregated form weakens the maximum absorption (Figure 2) [27].

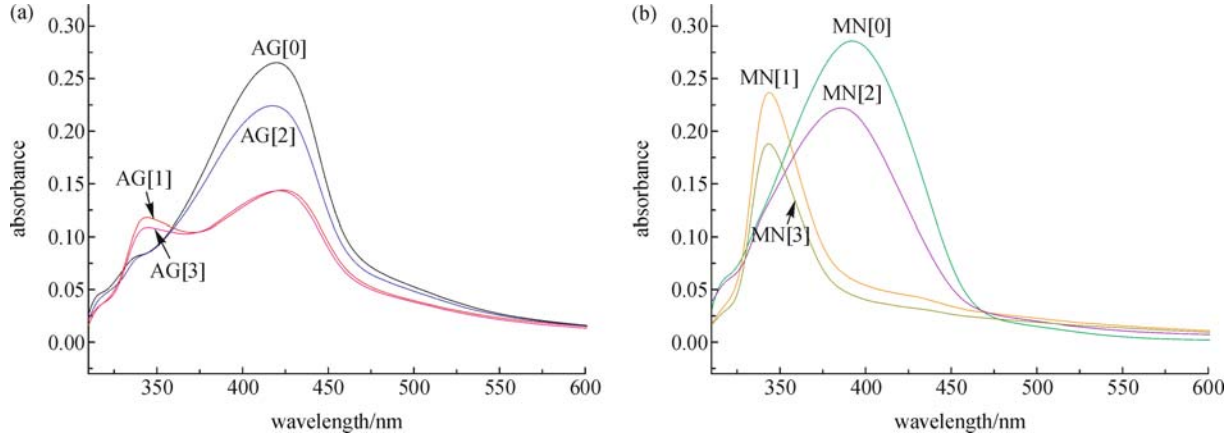

Figure 2 The absorption spectra of (a) the aggregated forms (left) and (b) the 1-Ada triggered monomeric forms (right) of DACD (3.0×10^{-5} M) in water at 288 K. The variations of the two groups of absorption curves fit an identical trend. The bare fluorophore out of the β-CD cavity can be fully protonized in the 1-Ada triggered monomeric forms so that the strong absorption peaks appear at 345 nm, while the original maximum absorption completely disappears.

Without the addition of 1-Ada, DACD chiefly adopts the aggregated state in each stable form (described using the TEM images in Figure 3 and the particle-size distribution characterization in Supporting Information, Figure A6). The protonation of the dimethylamino group easily weakens the inclusion of the cyclodextrin cavity to the fluorophore, leading to smaller aggregations (see the comparison of the TEM images and the particle-size characteristic of AG[1] to AG[0]). However, the influence on the aggregations of photoisomerization is little (see the comparison of the TEM images and particle-size characteristic of AG[2] to AG[0]). The ^{1}H-NMR spectra of these four forms are relatively fuzzy due to their sparing solubility in water. However, DACD becomes more solubilized in water with the addition of 1-Ada, which can be included in a β-CD cavity. The ^{1}H-NMR spectra for each 1-Ada triggered monomeric form (Supporting Information, Figure A8) show clearly dissociated DACD, indicating that the compound is soluble in D_2O. The peak shapes and their relative chemical shifts in the ^{1}H-NMR spectra of the MN[0] monomeric form are similar to those of DACD dispersed in DMSO-d6, while those of the MN[1] and MN[2] monomeric forms are like those of DACD stimulated by corresponding inputs in DMSO-d6 (see Supporting Information, Figure A7 and A8). This means that the protonation and the photoisomerization could also take place in water and that they can happen concurrently with the effect of 1-Ada. A new cluster of peaks in the ^{1}H-NMR spectra for MN[3] monomeric form appears compared to that for MN[1], indicating that both the two inputs worked effectively in this 1-Ada triggered stable state.

3.3 Address-crossing digital information processing

In this system, both the aggregated and the monomeric conformational stable species based on the simple

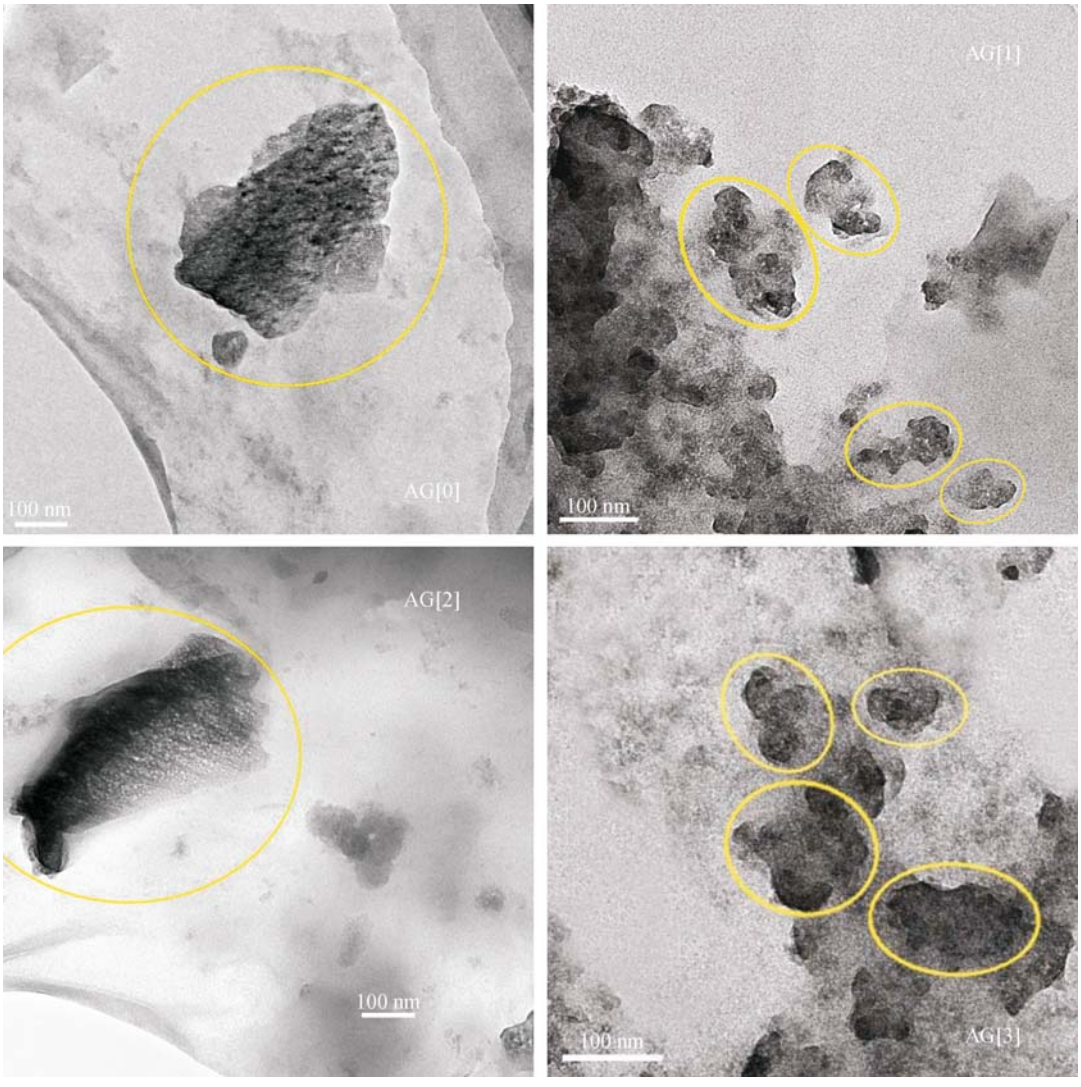

Figure 3 The image of the transmission electric microscopy (TEM) for each aggregated species of DACD. These solid samples were prepared from the corresponding conformational forms in water.

monomolecular platform are multi-responsive and can be used to record pH and UV signals. The aggregated and the 1-Ada triggered monomeric state, for their significant differences in the morphologies and the spectral characteristics, are assumed to share two different sequences of consecutive memory addresses (the aggregated AG and the monomeric MN series). Data access could be carried out from the sequence of the AG series address to the MN series with the aggregated state transforming to the monomeric state, and *vice versa*, by the simple chemical operations implemented by the addition or removal of 1-Ada. What's more, this address-crossing processing is reversible and repetitive (see Figure 1 and Scheme 3).

We define the original values in the initial aggregated and the monomeric forms as zero (the corresponding cell AG[0] = '00'; MN[0] = '00', Scheme 3). The memory cells of the AG and MN series addresses could record values when the external inputs are introduced. Here, cell AG[1] is assigned a value '01' in the absence of the light input and the presence of the pH input, and AG[2] = '10' in the presence of the light input but absence of the pH input. The cell AG[3] = '11' originates from the presence of both inputs. Another group of values in the MN series address for the monomeric state (MN[1] = '01', MN[2] = '10' and MN[3] = '11') is generated in the same way according to the signal inputs (Scheme 3). In these stable conformational species, the recorded pH and UV signals can be also erased by neutralization and heating, respectively. Unlike the components of a silicon-based computer, the data readout in nanosystems can be carried out at different modes, such as absorption, fluorescence (FL) [28–30], circular dichroism (CD) [31,32], and so on. The data recorded in the AG series can be read out by ICD signals

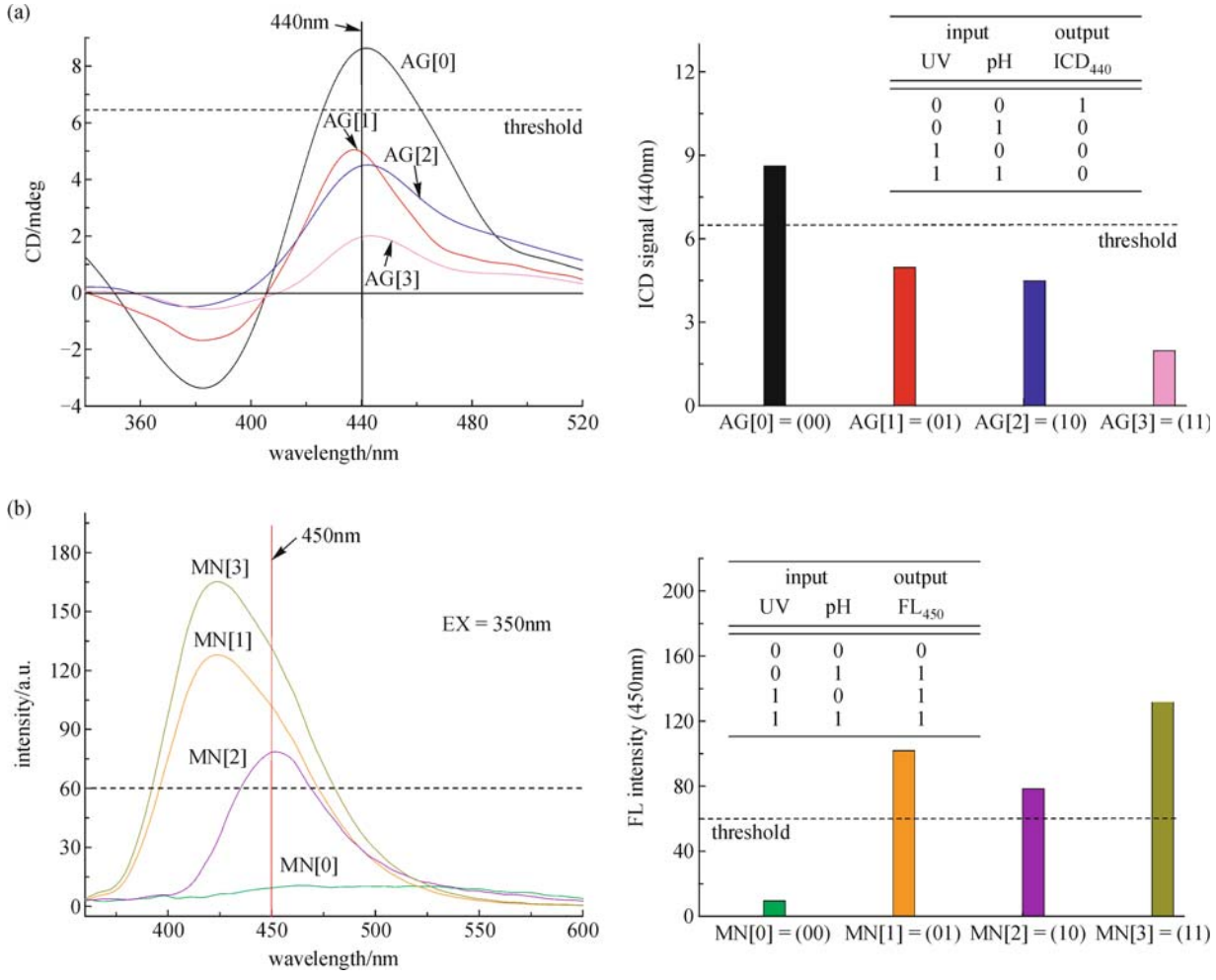

Figure 4 (a) (left) The ICD spectra of the aggregated forms of DACD (3.0×10^{-5} mol/L) in water at 288 K. (right) Bar graph representation of the NOR gate and the truth-table with the ICD signal at 440 nm as the output signal. The dash line represents the threshold (6.5 mdeg). (b) (left) The FL spectra of the 1-Ada triggered monomeric forms of DACD (3.0×10^{-5} mol/L) in water at 288 K; (right) Bar graph representation of the OR gate and the truth-table with the FL intensity at 450 nm as the output signal. The dash line represents the threshold (60).

because the aggregation enhanced the difference of the ICD signal and its unique characteristic, while the fluorescence signals for the MN series would be very sensitive and easy-to-communicative.

The D-π-A fluorophore of DACD is located in the chiral *β*-CD cavity in the aggregated state, so its π→π* and n→π* transitions, perpendicular to each other, would induce a strong negative Cotton effect at 380 nm and a positive Cotton effect at 440 nm, respectively. The input of pH change and light signals would affect the transition moments, or change their angle or position versus the *β*-CD axis, leading to decreases in the ICD signals [33, 34]. In this way, the data in the sequence of the AG series address can be read out with the CD mode, and a 'NOR' logic function can be integrated at an ICD signal output of 440 nm wavelength by setting up a certain threshold (Figure 4(a)). On the other hand, the 1-Ada triggered monomeric states show sensitive fluorescent-response for external inputs. The initial monomeric form shows a low fluorescent efficiency to an excitation at 350 nm. The photoisomerization of DACD would hinder the rotation of the dimethylanilino moiety by the steric factor of the aromatic rings in the *E*-isomer; hence, the radiative effect would be enhanced. The protonation of DACD may greatly hinder the fast quenching channel of the charge transfer in this twisted intramolecular charge-transfer (TICT) system [35], resulting in a larger blue-shifted emission peak. Therefore, the data in the sequence of the MN series can be read out in the fluorescent (FL) mode. Similarly, an 'OR' logic gate is demonstrated with the FL signal output at 450 nm wavelength by setting up a certain threshold (Figure 4(b)).

Totally, this nanosystem could mimic the functions of pointer-based data processing. In computer science, a pointer [36] is a data type whose value refers directly to (or 'points to') another data stored elsewhere in the memory using its address. If only an addressable pointer value points to the first address of an array (digit group) in a different sequence of the memory, it could achieve the digital information exchange between the arrays stored in the non-consecutive memory addresses on a compiling process. The switch between the aggregated and the monomeric state in this system is similar to the pointer operations since these memory media alternate their addresses for data writing and readout. The data here stored in the AG and MN series addresses can be regarded as two arrays. Although the 1-Ada-triggered switching can also work even as the pH or UV information exists, we mainly describe the switching between the initial aggregated and the monomeric forms, as the pointer operations point to the first address of the arrays AG[0] and MN[0], followed by information storage and logic calculations (see Scheme 3).

4 Conclusion

In summary, a self-aggregatable cyclodextrin derivative based effective digital information switching system, capable of data memories and logic functions, has been demonstrated in nanoscale. The address-crossing data processing was realized by a method analogous with pointer-operations, taking advantage of simple chemical operations. However, problems such as ion accumulations, low response speed, and incompleteness of conformational transformations should be overcome step by step. Although there is still a long way to go before this chemical system can be transformed to a practical

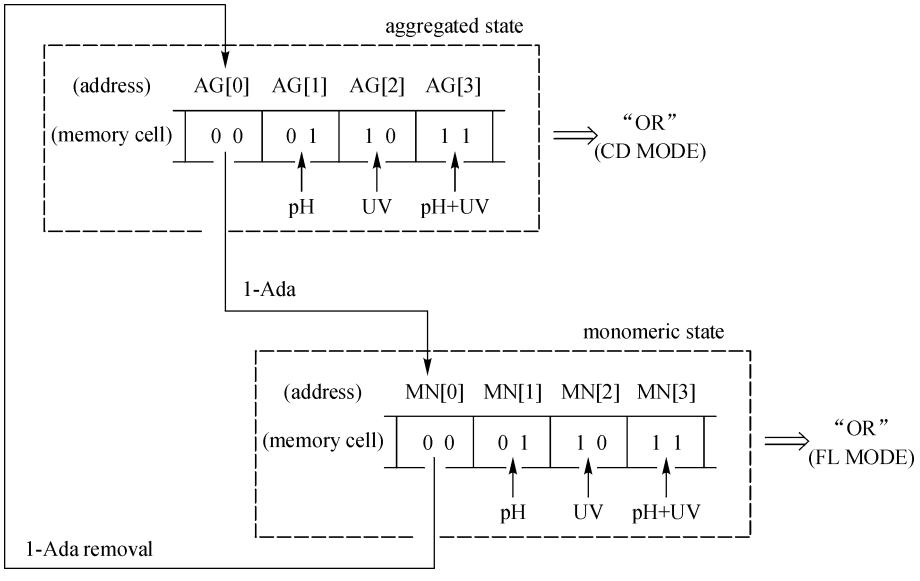

Scheme 3 Address-crossing operation scheme between the aggregated and the monomeric memory media, as well as the data writing and readout scheme in this system.

digital switching device, our next goal is to develop a communication network with this notion, in which the supramolecule can be well controlled by changing the external environment or stimuli accompanied by a coherent signal readout.

Acknowledgements The authors thank Prof. Jun-Po He at the Department of Macromolecule Science of Fudan University for the characterization of the self-assembly aggregated states. This work was financially supported by the National Natural Science Foundation of China (Grant Nos. 50673025, 20603009), the National Basic Research Program of China (Grant No. 2006CB806200) and partially by Scientific Committee of Shanghai.

Liangliang ZHU was born in 1982. He received the Bachelor's degree at the Department of Chemistry, Zhejiang University, Hangzhou, China in 2005. Now he is studying for the Ph. D. degree in applied chemistry at East China University of Science & Technology, Shanghai, China. His research interests mainly focused on the development of supramolecular functional materials and molecular machines.

Appendix: Synthetic procedures

4-(cyanomethyl)phenyl acetate (A1)

A stirred mixture of 2-(4-hydroxyphenyl)acetonitrile (10 g, 75.1 mmol) and conc. sulfuric acid (0.2 mL) dissolved into acetic anhydride(100 mL) was heated to 100°C for 3hrs under argon, cooled and poured into ice water (350 mL) slowly with stirring. Sodium carbonate was added to neutralize the solution and it was extracted twice with ethyl acetate (200 mL). After concentrated in vacuo, petroleum ether (150 mL) was added and a great deal of white solid A1 (13 g, 98.8%) was crystallized from the solution. M.p. 42–43°C.

^{1}H-NMR (400 MHz, $CDCl_3$, 25 °C, TMS): δ = 7.35(d, J = 8.4 Hz, 2H), 7.12(d, J = 8.8 Hz, 2H), 3.75(s, 2H), 2.31(s, 3H)

(Z)-3-(4-(dimethylamino)phenyl)-2-(4-hydroxyphenyl) acrylonitrile (A2)

A1 (3.8 g, 18.8 mmol), 4-dimethylamino benzaldehyde (2.8 g, 18.8 mmol) and DBU (3.2 g, 18.8 mmol) were dissolved in

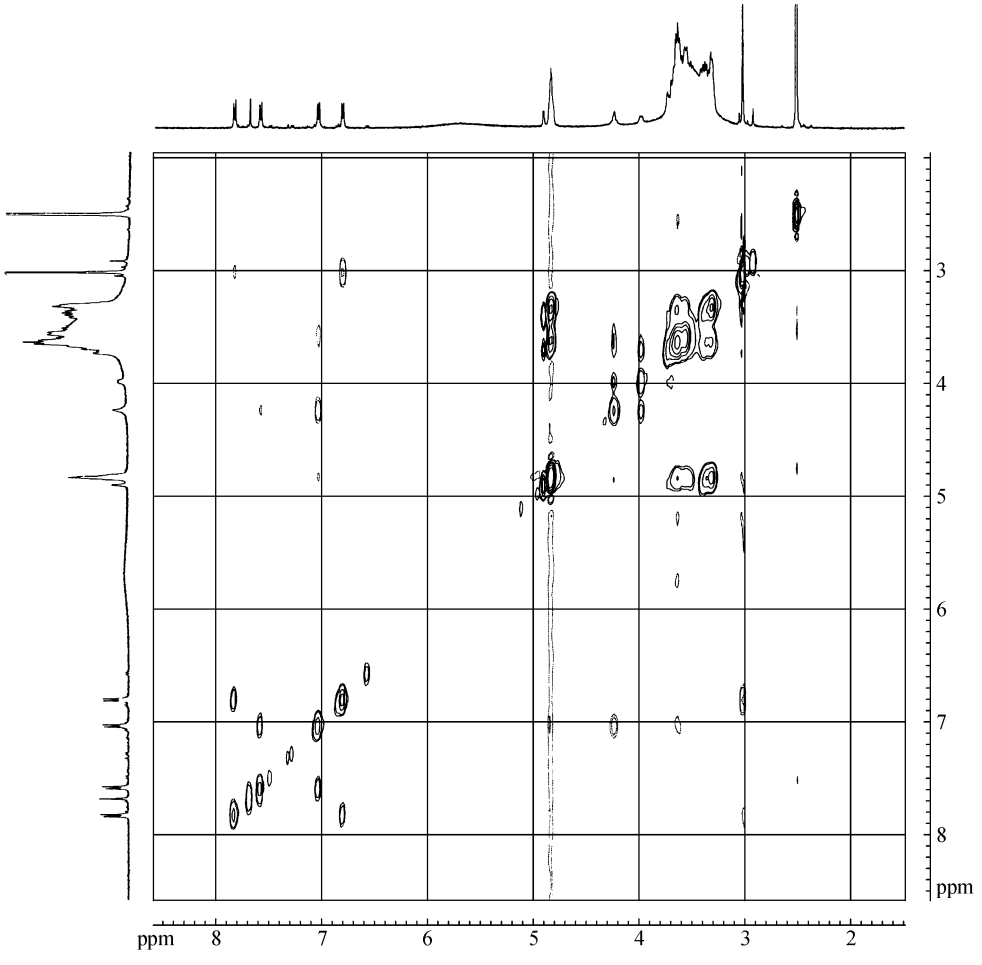

Figure A1 Two-dimensional ROESY NMR spectrum of DACD (500 MHz in DMSO-d6 at 298 K) after a mixing time of 300 ms.

pyridine (20 mL) and stirred for 18 h at 100°C under argon, then cooled, poured into de-ionized water (150 mL). Here the product had hydrolyzed to be a corresponding phenol. The solution was extracted three times with dichloromethane (150 mL) and the underlayer was washed with water (80 mL). After drying with anhydrous $MgSO_4$ and concentrated in vacuo, the residue was applied to silica gel chromatography (petroleum ether : ethyl acetate = 5:1) and washed with hexane/CCl4 = 2:1 to afford yellow compound A2 (4.1g, 82%). M.p. 214–215°C.

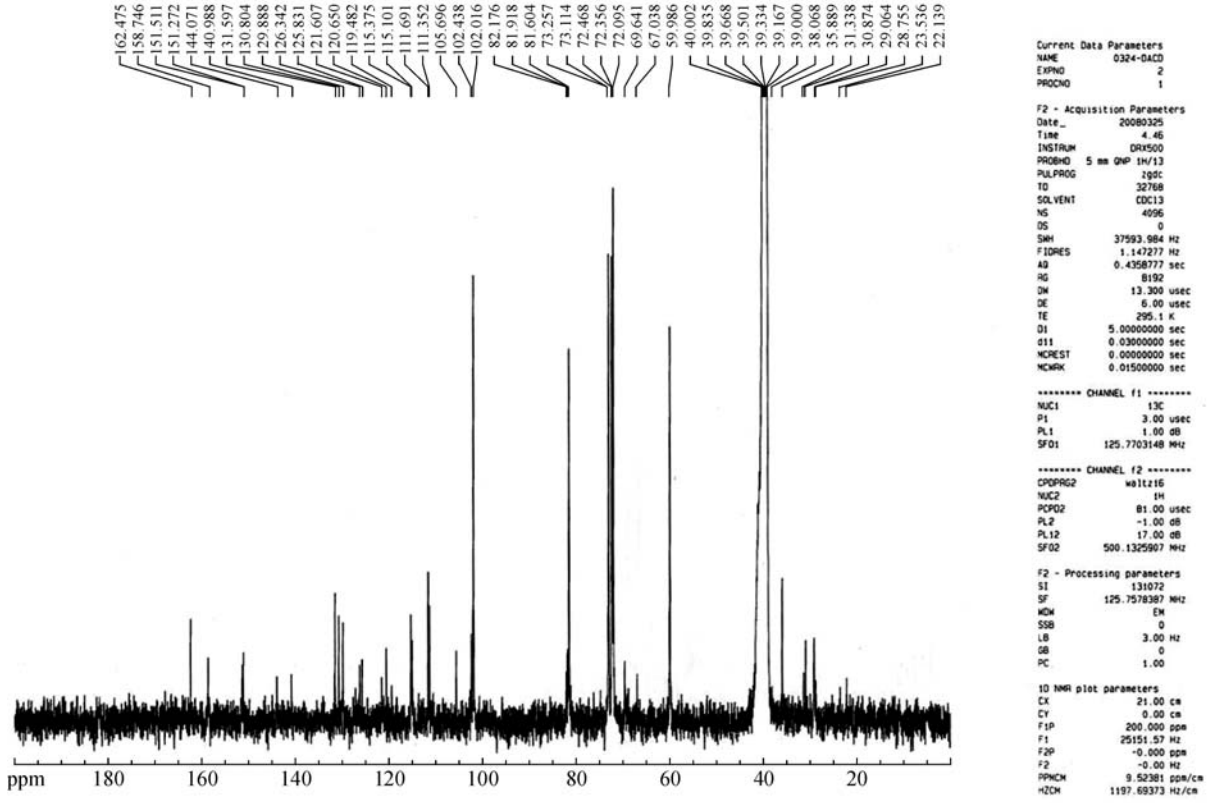

Figure A2 ^{13}C NMR spectrum of DACD in DMSO-d6 (500 MHz).

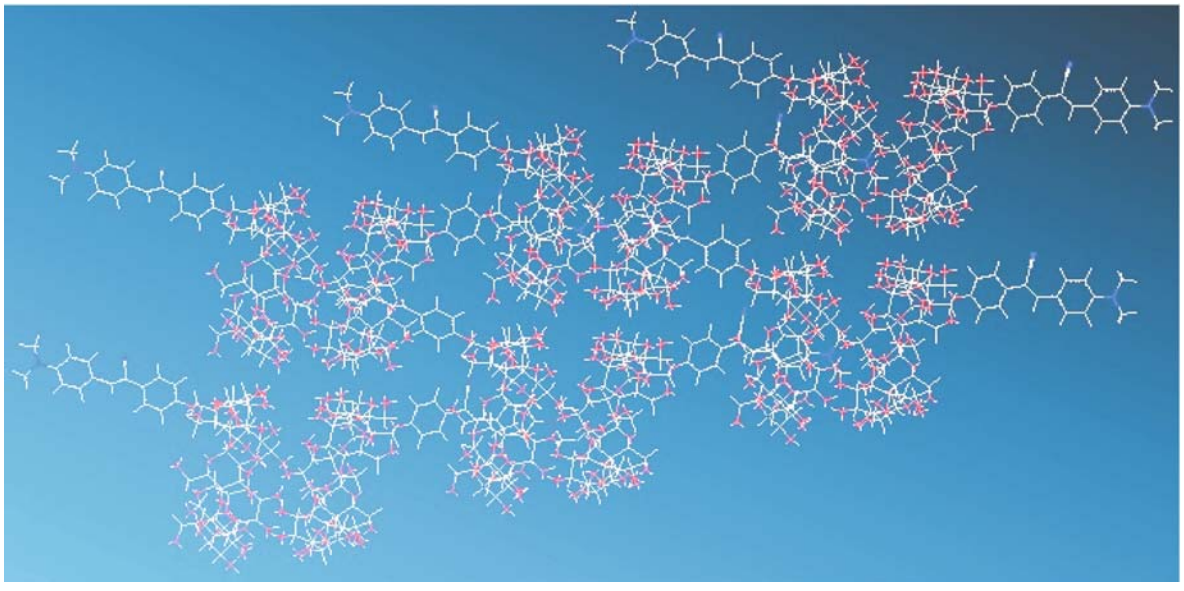

Figure A3 Part of the proposed aggregated layer structure optimized by molecular mechanics (MM2).

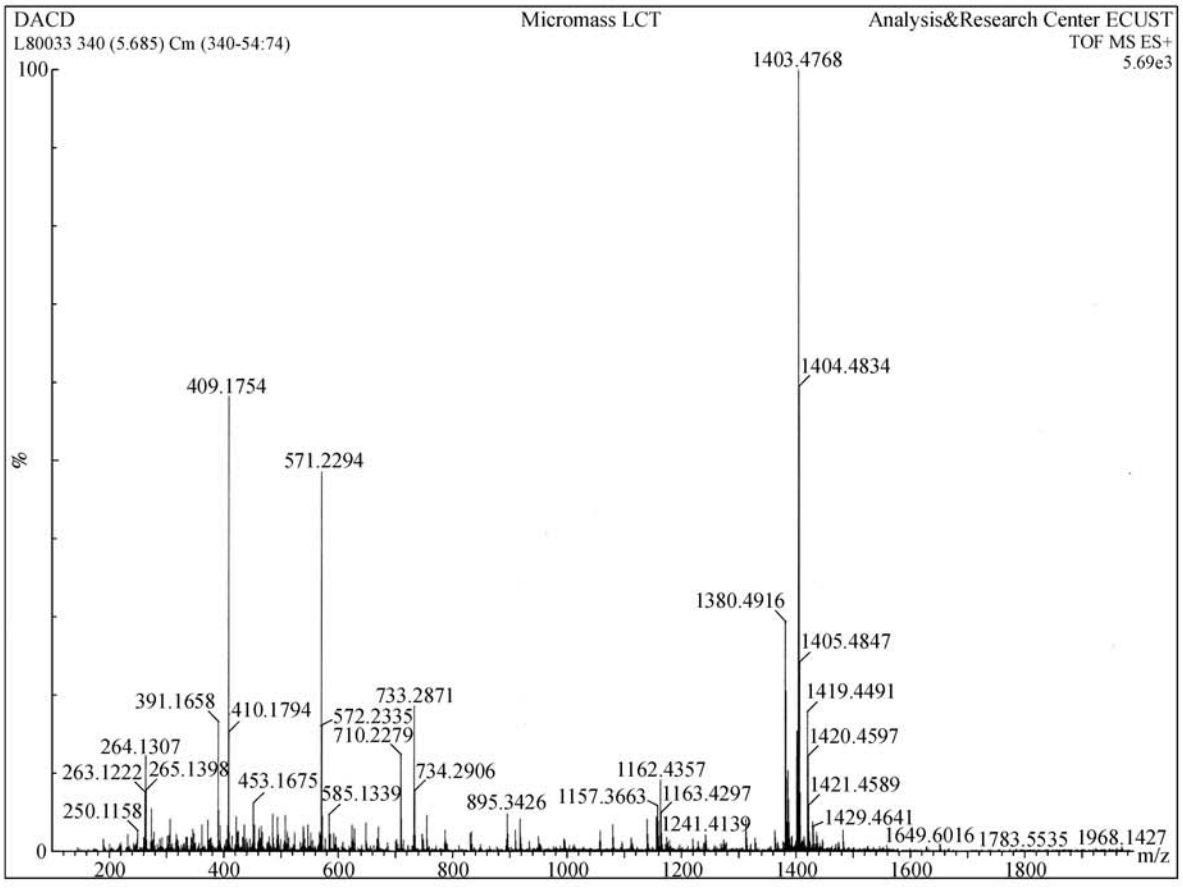

Elemental Composition Report

Multiple Mass Analysis: 3 mass(es) processed

Tolerance = 5.0 mDa / DBE: min = −20.0, max = 100.0

Isotope cluster parameters: Separation = 1.0 Abundance = 1.0%

Monoisotopic Mass, Odd and Even Electron Ions

17 formula(e) evaluated with 2 results within limits (up to 50 closest results for each mass)

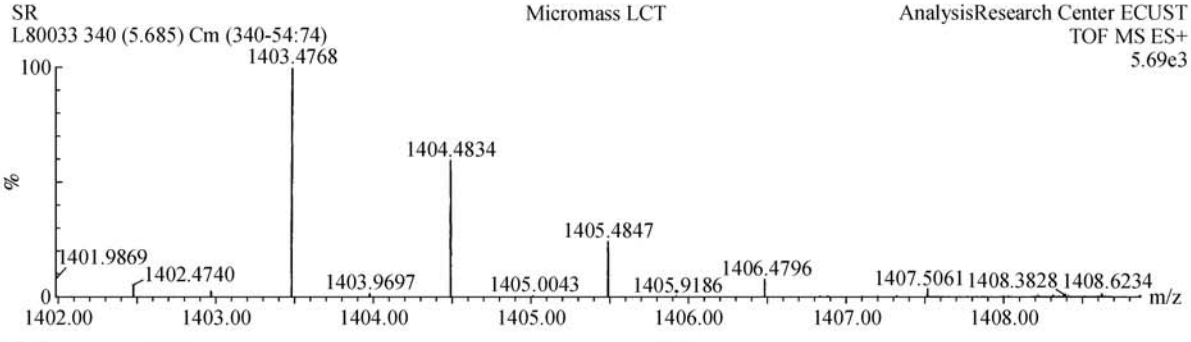

Minimum:	15.00				−20.0					
Maximum:	100.00		5.0	5.0	100.00					
Mass	RA	Calc.Mass	mDa	PPM	DBE	Score	Formula			
1403.4768	100.00	1403.4752	1.6	1.1	18.5	n/a	12C59 23Na	1H84 14N2	16035	
1404.4834	59.53	1404.4786	4.8	3.4	18.5	n/a	12C58 23Na	13C 14N2	1H84	16035
1405.4847	24.15									

Figure A4 HRMS (ESI) spectrum of DACD.

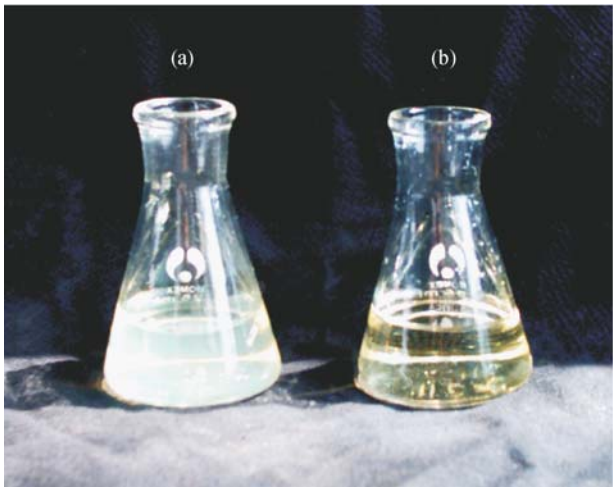

Figure A5 The image of DACD dispersed in water (a) and in DMF (b) photoed under sunlight ($3.0\times10-5$ mol/L).

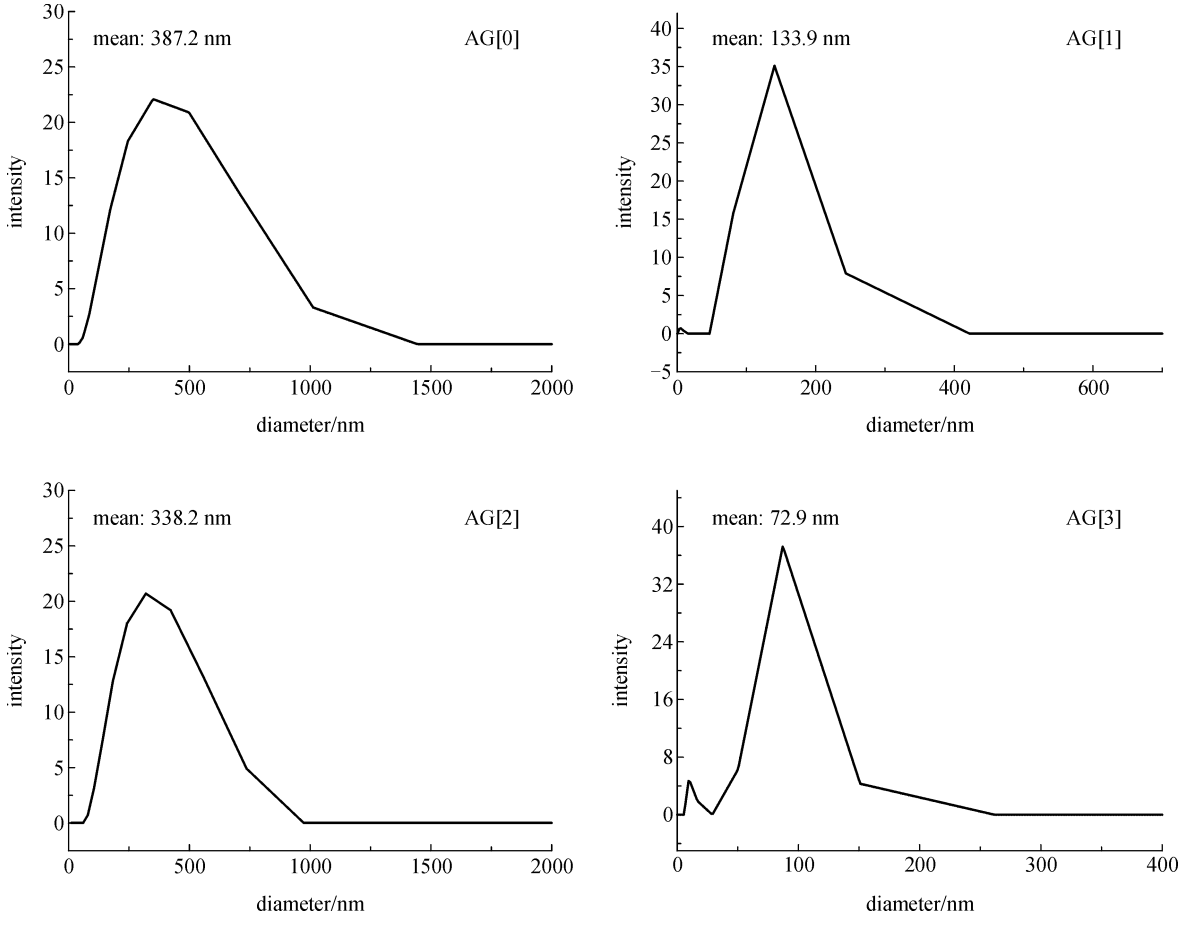

Figure A6 The particle-size distribution for each aggregated species of DACD in water ($3.0\times$10-5 mol/L, 288K).

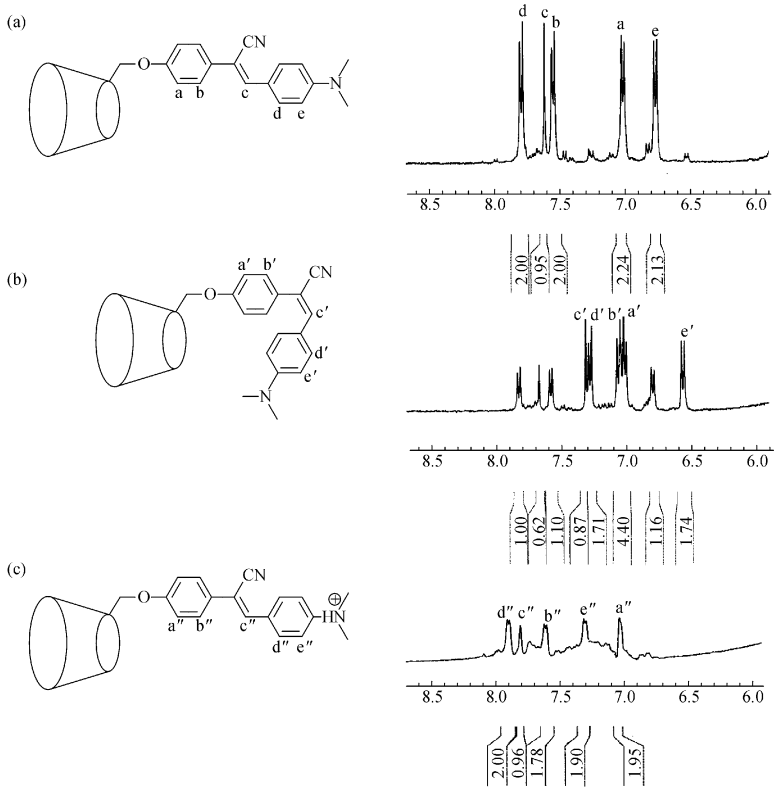

Figure A7 Low field ^{1}H NMR spectra (400 MHz in DMSO-d6 at 298 K) of DACD (a) of the initial structure, (b) fully irradiated at 380 nm and (c) fully protonated by conc. HCl.

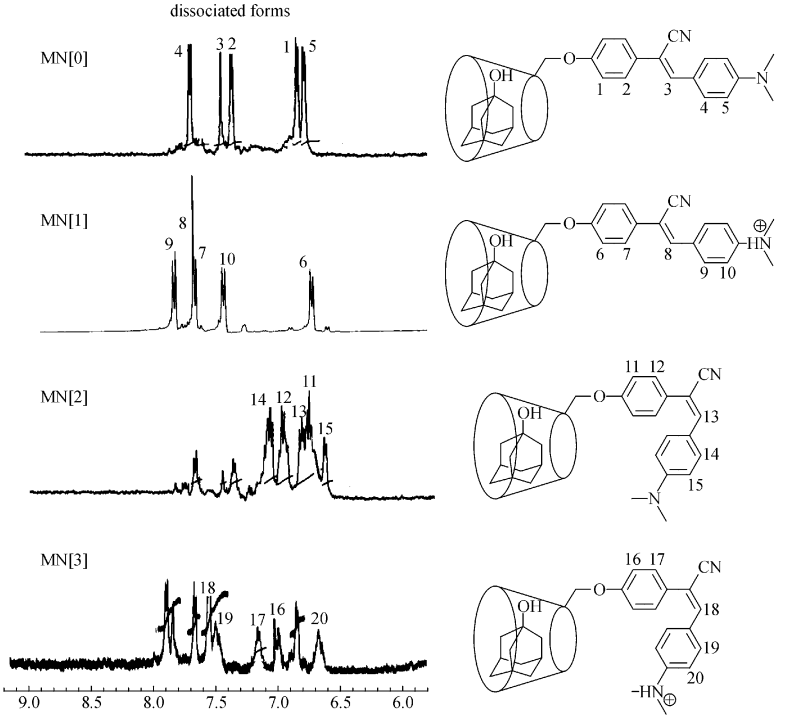

Figure A8 Low field ^{1}H NMR spectra (400 MHz in D2O at 298 K) for each 1-Ada triggered monomeric species of DACD. Because of the sparing water-solubility of the aggregations, the quality of the ^{1}H NMR spectra for the aggregated species is very low.

^{1}H-NMR (400 MHz, $CDCl_3$, 25°C, TMS): δ = 7.83(d, J = 8.4 Hz, 2H), 7.51(d, J = 8.0 Hz, 2H), 7.30(s, 1H), 6.89(d, J = 8.0 Hz, 2H), 6.72(d, J = 8.4 Hz, 2H), 3.06(s, 6H)

Mono(6-O-p-Toluenesulfonyl)-β-cyclodextrin(B)

This compound was prepared as described by Byun, Zhong and Bittman [37] (14.7 g, 9.7%). M.p. 185°C (decomp).

^{1}H-NMR (400 MHz, DMSO-d6, 25 °C, TMS): δ = 7.73(d, J = 8.4 Hz, 2H), 7.42(d, J = 8.4 Hz, 2H), 5.61–5.81(m, 14H), 4.81(m, 5H), 4.75(m, 2H), 4.42–4.58(m, 5H), 4.29–4.39(m, 2H), 4.20(m, 1H), 3.15–3.72 (m), 2.41s, 3H)

Association constant K between DACD and 1-Ada [38]

The association constant between DACD and 1-Ada in aqueous solution was determined by following the UV absorption at 430 nm. The concentration of DACD was kept at 3×10^{-5} mol/L. Upon addition of excess 1-Ada, the absorption at 430 nm decreased remarkably. With an assumption of a 1:1 stoichiometry, the inclusion complexation is expressed by the following equation:

$$[\text{DACD}]+[\text{1-Ada}] \overset{\text{K}}{\rightleftharpoons} [\text{DACD}\cdot\text{1-Ada}]$$

We employed the usual double reciprocal plot according to the modified Hidebrand-Benesi equation:

$$1/[\Delta A] = 1/K[\Delta\varepsilon][\text{DACD}][\text{1-Ada}]+1/[\Delta\varepsilon][\text{DACD}]$$

where [DACD] and [1-Ada] denote the initial concentrations DACD and 1-Ada, respectively. Using the nonlinear least squares curve-fitting method, we obtained the association constant ($K = 1.09\times10^4$ (mol/L)$^{-1}$) for this system.

References

1. Balzani, V.; Credi, A.; Raymo, F. M.; Stoddart, J. F., *Angew. Chem. Int. Ed*. **2000**, *39*, 3348
2. Tian, H.; Wang, Q. C., *Chem. Soc. Rev*. **2006**, *35*, 361
3. Kay, E. R.; Leigh, D. A.; Zerbetto, F., *Angew. Chem. Int. Ed*. **2007**, *46*, 72
4. Klotz, E. J. F.; Claridge, T. D. W.; Anderson, H. L., *J. Am. Chem. Soc*. **2006**, *128*, 15374
5. Green, J. E.; Choi, J. W.; Boukai, A.; Bunimovich, Y.; Johnston-Halperin, E.; Delonno, E.; Luo, Y.; Sheriff, B. A.; Xu, K.; Shin, Y. S., Tseng, H. R.; Stoddart, J. F.; Heath, J. R., *Nature* **2007**, *445*, 414
6. Niazov, T.; Baron, R.; Katz, E.; Lioubashevski, O.; Willner, I., *Proc. Natl. Acad. Sci. U. S. A*. **2006**, *103*, 17160
7. Raymo, F. M., *Adv. Mater*. **2002**, *14*, 401
8. Ballardini, R.; Ceroni, P.; Credi, A.; Gandolfi, M. T.; Maestri, M.; Semararo, M.; Venturi, M.; Balzani, V., *Adv. Funct. Mater*. **2007**, *17*, 740
9. Liu, Y.; Chen, Y., *Acc. Chem. Res*. **2006**, *39*, 681
10. Wenz, G.; Han, B. H.; Müller, A., *Chem. Rev*. **2006**, *106*, 782
11. Ma, X.; Qu, D. H.; Ji, F. Y.; Wang, Q. C.; Zhu, L. L.; Xu, Y.; Tian, H., *Chem. Commun*. **2007**, 1409
12. Wang Y.; Ma N.; Wang Z.; Zhang, X., *Angew. Chem. Int. Ed*. **2007**, *46*, 2823
13. Zhou Y. C.; Wu H.; Qu L.; Zhang D. Q.; Zhu D. B., *J. Phys. Chem. B* **2006**, *110*, 15676
14. Browne W. R.; Pollard M. M.; de Lange B.; Meetsma A.; Feringa B. L., *J. Am. Chem. Soc*. **2006**, *128*, 12412
15. Tian, H.; Qin, B.; Yao, R. X.; Zhao, X. L.; Yang, S. J., *Adv. Mater*. **2003**, *15*, 2104
16. Gupta T.; van der Boom M. E., *Angew. Chem. Int. Ed*. **2008**, *47*, 5322
17. Qu, D. H.; Ji, F. Y.; Wang, Q. C.; Tian, H., *Adv. Mater*. **2006**, *18*, 2035
18. Qu, D. H.; Wang, Q. C.; Tian, H., *Angew. Chem., Int. Ed*. **2005**, *44*, 5296
19. Margulies, D.; Melman, G.; Shanzer, A., *J. Am. Chem. Soc*. **2006**, *128*, 4865
20. Guo, Z. Q.; Zhu, W. H.; Shen, L. J.; Tian, H., *Angew. Chem. Int. Ed*. **2007**, *46*, 5549
21. Strack, G.; Ornatska, M.; Pita, M.; Katz, E., *J. Am. Chem. Soc*. **2008**, *130*, 4234
22. Andréasson, J.; Straight S. D. ; Bandyopadhyay, S.; Mitchell, R. H.; Moore, T. A.; Moore, A. L.; Gust, D., *Angew. Chem., Int. Ed*. **2007**, *46*, 958
23. Distinct Cotton effects occur at 380 nm and 440 nm, but monomeric states of DACD scarcely generate ICD signal in DMF.
24. Since the binding constant (1.09×10^4 mol/L^{-1}) between 1-Ada and DACD is so big, it will need much organic solvent to remove 1-Ada. This process is implemented by washing the DACD system with seven-fold n-hexane and then removing the residual n-hexane under reduced pressure.
25. Ueno A.; Kuwabara T.; Nakamura A.; Toda F., *Nature* **1992**, *356*, 136
26. Zhang D.; Su J.-H.; Ma X.; Tian H., *Tetrahedron*, **2008**, *64*, 8515
27. Trans-to-cis photoisomerization of azobenzene or stilbene compounds are generally accompanied by a decrease in maximum absorption. For example: Qu, D. H.; Wang, Q. C.; Ren, J.; Tian, H., *Org. Lett*. **2004**, *6*, 2085
28. Wang, Q. C.; Qu, D. H.; Ren, J.; Chen, K.C.; Tian, H., *Angew. Chem. Int. Ed*. **2004**, *43*, 2661
29. Pérez, E. M.; Dryden, D. T. F.; Leigh, D. A.; Teobaldi, G.; Zerbetto, F. A., *J. Am. Chem. Soc*. **2004**, *126*, 12210
30. Zhu, L.L.; Li X.; Ji, F. Y.; Ma, X.; Wang, Q. C.; Tian, H., *Langmuir* **2009**, *25*, 3482
31. Berova, N.; Bari, L. D.; Pescitelli, G., *Chem. Soc. Rev.*, **2007**, *36*, 914
32. Ma, X.; Wang, Q. C.; Qu, D. H.; Xu, Y.; Ji, F. Y.; Tian, H., *Adv. Funct. Mater*. **2007**, *17*, 829

33. Kodaka, M., *J. Phys. Chem. A* **1998**, *102*, 8101
34. Zhu, L.L.; Ma, X.; Ji, F. Y.; Wang, Q. C.; Tian, H., *Chem. Eur. J.* **2007**, *13*, 9216
35. Grabowski Z. R.; Rotkiewicz K.; Rettig W., *Chem. Rev*. **2003**, *103*, 3899
36. Plauger P. J.; Brodie J., *ANSI and ISO Standard C Programmer's Reference* Microsoft Press, 1992
37. H. S. Byun; N. Zhong; R. Bittman, *Org. Synth.* **2000**, *77*, 225
38. H. A. Benesi; J. H. Hildebrand, *J. Am. Chem. Soc*. **1949**, *71*, 2703